

Non-iterative Wide-modulation-index Switching-angle Calculation Techniques for 15-level Binary Cascaded H-bridge Multilevel Inverter

J. A. Soo¹, M. S. Chye², Y. C. Tan³, S. L. Ong⁴, J. H. Leong⁵, T. Sutikno⁶

^{1-3,5}CERE/EMAD/PECO, School of Electrical Systems Engineering, University Malaysia Perlis, Malaysia

⁴School of Microelectronic Engineering, University Malaysia Perlis, Malaysia

⁶Electrical Engineering Department, Universitas Ahmad Dahlan, Indonesia

Article Info

Article history:

Received Sep 26, 2016

Revised Dec 02, 2016

Accepted Dec 12, 2016

Keyword:

Asymmetric multilevel inverter

Binary multilevel inverter

Cascaded H-Bridge

Multilevel inverter

Non-Iterative

ABSTRACT

Cascaded H-bridge multilevel inverter (CHBMI) is able to generate a staircase AC output voltage with low switching losses. The switching angles applied to the CHBMI have to be calculated and arranged properly in order to minimize the total harmonic distortion (THD) of the output voltage waveform. In this paper, two non-iterative switching-angle calculation techniques applied for a 15-level binary asymmetric CHBMI are proposed. Both techniques employ a geometric approach to estimate the switching angles, and therefore, the generated equations can be solved directly without iterations, which are usually time-consuming and challenging to be implemented in real-time. Apart from this, both techniques are also able to calculate the switching angles for a wide range of modulation index. The proposed calculation techniques have been validated via MATLAB simulation and experiment.

Copyright © 2017 Institute of Advanced Engineering and Science.
All rights reserved.

Corresponding Author:

J. A. Soo,
School of Electrical Systems Engineering,
University Malaysia Perlis,
02600 Arau, Perlis, Malaysia.
Email: soo.edmund@gmail.com

1. INTRODUCTION

Cascaded H-bridge multilevel inverter (CHBMI) has drawn increased attention in recent decades owing to its modularity and low switching losses [1]-[4]. There are two categories of CHBMI: (a) symmetric and (b) asymmetric. In symmetric CHBMI, the DC source voltages in all HBs are identical whilst asymmetrical CHBMI has difference DC source voltage levels. For a given number of HB, an asymmetric CHBMI is able to produce a staircase AC output voltage waveform with a higher number of voltage level than that of a symmetric CHBMI [5]-[8]. Generally, a staircase AC output voltage waveform with a higher number of voltage level is expected to produce lower total harmonic distortion (THD). However, the THD of the staircase AC output voltage waveform can become very high if the switching angles are not properly arranged [3]. Conventionally, a set of non-linear transcendental equations involving trigonometric equations has to be solved to obtain the switching angles. In [9]-[11], iterative methods are employed to solve these non-linear transcendental equations. However, solving these equations using iterative methods can be time-consuming and challenging to be performed in real-time. Moreover, if the initial conditions of the switching angles are not correctly chosen, the number of iteration cycles can be very large and the algorithm may fail to converge, leading to no solutions. In [12], the author proposed two non-iterative methods to estimate the switching angles according to the sine function. However, the methods employed in [12] can only calculate the switching angles at a specific modulation index, and thereby cannot be applied directly in applications that require a wider modulation index range. In this paper, two non-iterative switching angle calculation

techniques for a 15-level binary asymmetric CHBMI are proposed. The techniques are able to calculate the switching angles for a wide range of modulation index. Both techniques have been validated via MATLAB simulation and experimental results.

2. PROPOSED SWITCHING ANGLE CALCULATION TECHNIQUE

In [6], two non-iterative methods are presented. The first method calculates the switching angles at each interception point between a sine waveform and the half height of each stepped output voltage level, whilst in the second method the switching angles are calculated from half of the switching angles obtained using the first method. Since both methods employ geometry approach to estimate the switching angles, the generated equations can be solved directly. However, both methods are only able to estimate the switching angles at a specific modulation index. In this paper, both methods have been extended to enable the calculation of switching angles over a wide modulation index range applied to a 15-level binary asymmetric CHBMI. The proposed switching-angle calculation techniques, referred as CTA and CTB in this paper, are given in Equations 1 and 2, respectively.

$$\begin{aligned} \theta_1 &= \sin^{-1}\left(\frac{\pi}{56M_a}\right) & \theta_2 &= \sin^{-1}\left(\frac{3\pi}{56M_a}\right) & \theta_3 &= \sin^{-1}\left(\frac{5\pi}{56M_a}\right) & \theta_4 &= \sin^{-1}\left(\frac{7\pi}{56M_a}\right) \\ \theta_5 &= \sin^{-1}\left(\frac{9\pi}{56M_a}\right) & \theta_6 &= \sin^{-1}\left(\frac{11\pi}{56M_a}\right) & \theta_7 &= \sin^{-1}\left(\frac{13\pi}{56M_a}\right) \end{aligned} \quad (1)$$

$$\begin{aligned} \theta_1 &= \frac{1}{2} \sin^{-1}\left(\frac{\pi}{56M_a}\right) & \theta_2 &= \frac{1}{2} \sin^{-1}\left(\frac{3\pi}{56M_a}\right) & \theta_3 &= \frac{1}{2} \sin^{-1}\left(\frac{5\pi}{56M_a}\right) & \theta_4 &= \frac{1}{2} \sin^{-1}\left(\frac{7\pi}{56M_a}\right) \\ \theta_5 &= \frac{1}{2} \sin^{-1}\left(\frac{9\pi}{56M_a}\right) & \theta_6 &= \frac{1}{2} \sin^{-1}\left(\frac{11\pi}{56M_a}\right) & \theta_7 &= \frac{1}{2} \sin^{-1}\left(\frac{13\pi}{56M_a}\right) \end{aligned} \quad (2)$$

where $\theta_1, \theta_2, \theta_3, \theta_4, \theta_5, \theta_6$ and θ_7 are switching angles. The modulation index (M_a) in Equations 1 and 2 is given by

$$M_a = \frac{\pi V_1}{28V_{DC}} \quad (3)$$

$$V_1 = \frac{4V_{DC}}{\pi} [\cos(\theta_1) + \cos(\theta_2) + \cos(\theta_3) + \cos(\theta_4) + \cos(\theta_5) + \cos(\theta_6) + \cos(\theta_7)] \quad (4)$$

where V_1 is the fundamental voltage of the staircase AC output voltage waveform which can be calculated using Equation 4, and V_{DC} is the magnitude of each stepped output voltage level.

3. SWITCHING PATTERN OF 15-LEVEL BINARY ASYMMETRIC CASCADED H-BRIDGE MULTILEVEL INVERTER

Figure 1(a) shows the asymmetric CHBMI with the DC source voltage levels increase in a binary fashion. The total number of the inverter output voltage level (m) is dependent on the total number (s) of independent DC source which can be determined by

$$m = 2^{s+1} - 1 \quad (5)$$

Each effective output voltage level (V_{DC-i}) respective to i -th switching angle (θ_i) at the first quadrant of the CHBMI is given by

$$V_{DC-i} = \frac{14 i V_{DC}}{m-1} \quad (6)$$

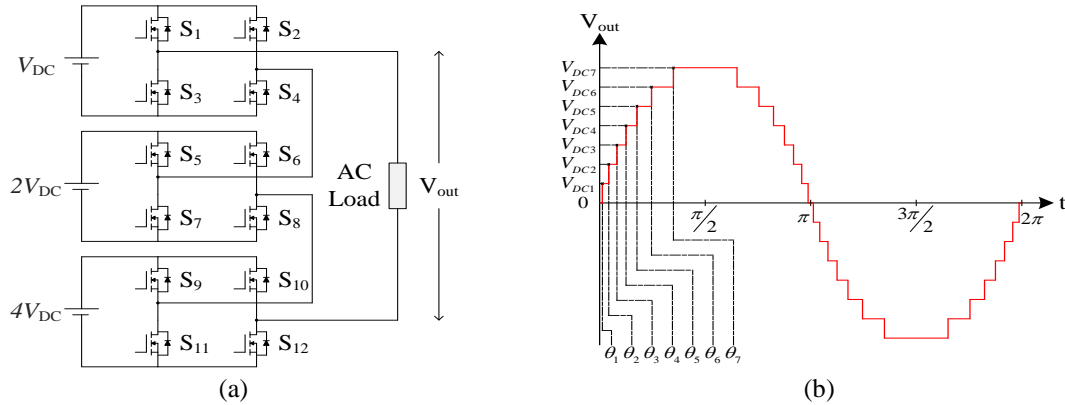


Figure 1. (a) Block diagram of 15-level binary asymmetric CHBMI
(b) Output voltage waveform of 15-level binary asymmetric CHBMI

Table 1. Switching Pattern of 15-level Binary Asymmetric CHBMI

Output Level (V)	HB DC Source (V)			Switches											
	V_{DC}	$2V_{DC}$	$4V_{DC}$	S1	S2	S3	S4	S5	S6	S7	S8	S9	S10	S11	S12
$7V_{DC}$	✓	✓	✓	1	0	0	1	1	0	0	1	1	0	0	1
$6V_{DC}$		✓	✓	1	1	0	0	1	0	0	1	1	0	0	1
$5V_{DC}$	✓		✓	1	0	0	1	1	1	0	0	1	0	0	1
$4V_{DC}$			✓	0	0	1	1	0	0	1	1	1	0	0	1
$3V_{DC}$	✓	✓		1	0	0	1	1	0	0	1	1	1	0	0
$2V_{DC}$		✓		1	1	0	0	1	0	0	1	1	1	0	0
V_{DC}	✓			1	0	0	1	1	1	0	0	1	1	0	0
0				0	0	1	1	0	0	1	1	0	0	1	1
$-V_{DC}$	✓			0	1	1	0	0	0	1	1	0	0	1	1
$-2V_{DC}$		✓		0	0	1	1	0	1	1	0	0	0	1	1
$-3V_{DC}$	✓	✓		0	1	1	0	0	1	1	0	0	0	1	1
$-4V_{DC}$			✓	1	1	0	0	1	1	0	0	0	1	1	0
$-5V_{DC}$	✓		✓	0	1	1	0	1	1	0	0	0	1	1	0
$-6V_{DC}$		✓	✓	1	1	0	0	0	1	1	0	0	1	1	0
$-7V_{DC}$	✓	✓	✓	0	1	1	0	0	1	1	0	0	1	1	0

Note: "0" is OFF, "1" is ON

The switching pattern of a 15-level binary asymmetric CHBMI respective to each stepped output voltage level is shown in Table 1. The highest output voltage level of the inverter is V_{DC7} which is the sum of the independent DC sources ($V_{DC} + 2V_{DC} + 4V_{DC}$). Since the output voltage waveform of the inverter possesses the characteristic of half-wave symmetry, only seven switching angles in the first quadrant are needed to be calculated. Each switching angle corresponds to each effective output voltage level as shown in Figure 1(b).

4. SIMULATION AND EXPERIMENTAL RESULTS

Table 2 shows the parameters used in the simulation and experimental setup for a 15-level binary asymmetric CHBMI. The inverter consists of three HBs and the DC sources are set at 10V, 20V, and 40V, respectively. Twelve switches are used and switched at 50Hz. Figure 2 shows the MATLAB simulation results calculated using CTA and CTB. The THD is computed by

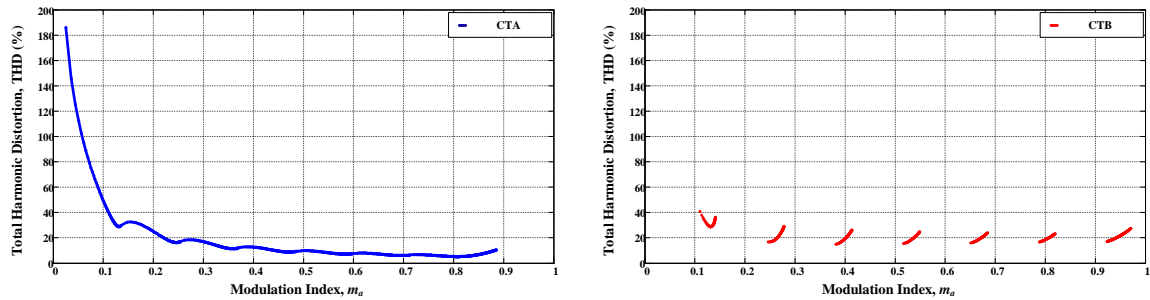
$$THD = \frac{\sqrt{\sum_{n=2}^{\infty} V_n^2}}{V_1} \quad (7)$$

where V_n is the n -th harmonic of the output voltage waveform. Based on the simulation results shown in Figure 2, CTA and CTB are able to calculate the switching angles for a wider range of modulation index. The highest modulation index achievable for CTA and CTB are 0.89 and 0.97, respectively, whilst the lowest possible modulation index for CTA and CTB are 0.03 and 0.11, respectively. Besides, CTA is able to provide

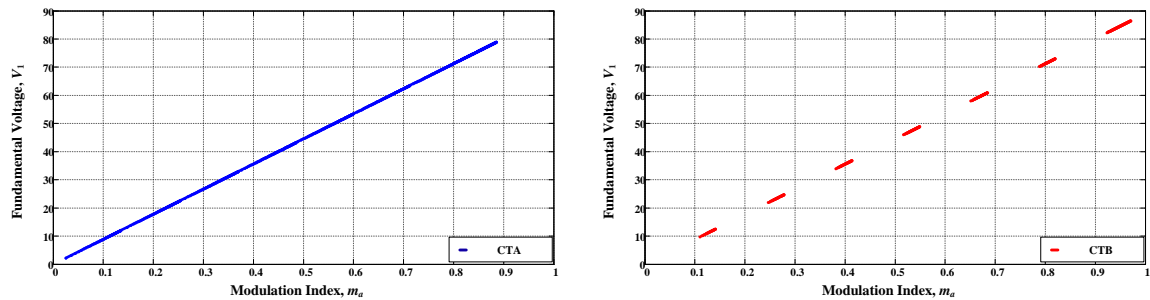
a continuous solution over a wide modulation index, whilst CTB is only able to give solution at certain intervals of modulation index. There is no solution at higher modulation index for CTA because the domain of the arcsine function is limited between -1~1 to generate the switching angles in real number. If a higher fundamental voltage is required, CTB can be considered as it is able to provide solutions at higher modulation index.

Table 2. Parameters used in Simulation and Experimental Setup

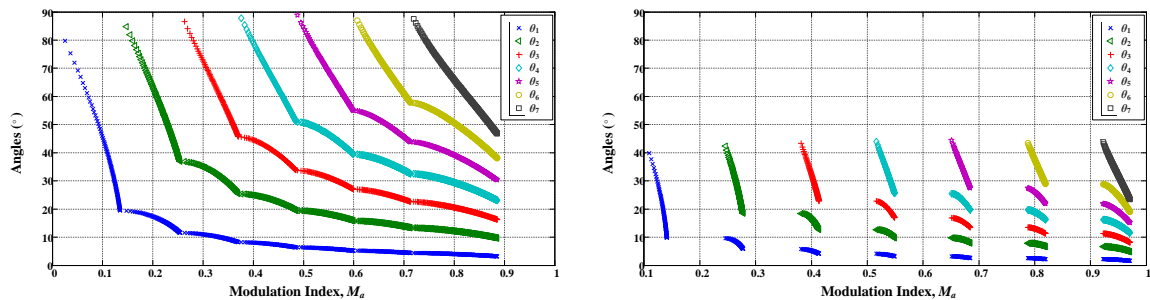
Parameters	Values
Number of HB	3
HB DC sources	10V, 20V, and 40V
Output Frequency	50Hz
Modulation Index Resolution	0.001



(a) THD against modulation index



(b) Fundamental voltage against modulation index



(c) Switching angles against modulation index

Figure 2. MATLAB simulation results of the proposed calculation techniques for 15-level binary asymmetric CHBMI

A 15-level binary asymmetric CHBMI prototype has been constructed as shown in Figure 3. The prototype is controlled using a Microchip PIC18F4550 microcontroller and twelve power MOSFET gate drivers. The HBs are powered by three independent DC power supplies i.e. 10V, 20V, and 40V,

respectively. Figures 4 and 5 show the experimental results of CTA and CTB for the inverter. At the same modulation index, both calculation techniques produce different waveforms and THD. The THD of the output voltage waveform for CTB is higher than the CTA. This is because the output voltage waveform has a narrower gap between positive half and negative half cycle compared to that of CTA, which resembles a sine wave closer. Furthermore, the narrower gap of the output voltage waveform approaching a square wave gives higher fundamental voltage but at the cost of higher THD. Besides that, the higher THD of the CTB is also attributed to the high third harmonic at 150Hz in the output voltage waveform. Table 3 compares the simulation and experimental data of both calculation techniques. The simulation and experimental results are in good agreement. The differences between the CTA and CTB can be clearly observed in Table 3 where the CTA has lower THD than the CTB at the same modulation index.

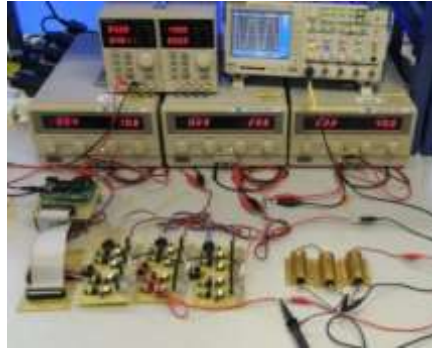
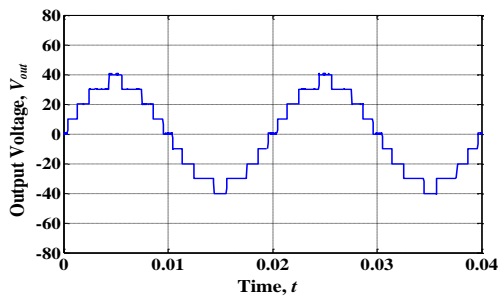
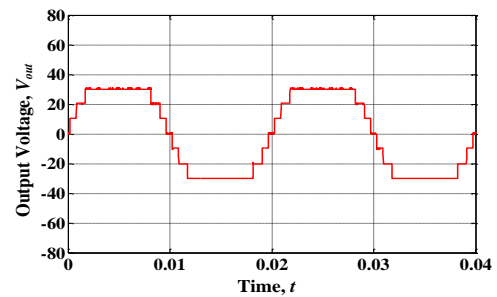


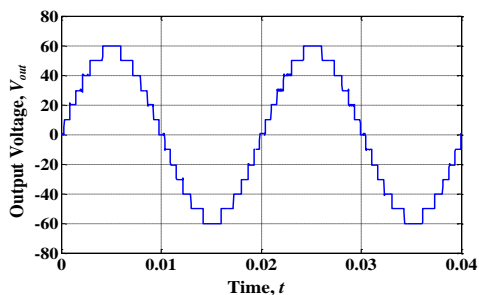
Figure 3. (a) 15-level binary asymmetric CHBMI experiment setup



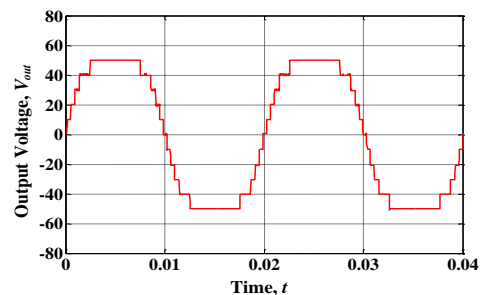
(a) CTA at $m_a = 0.40$



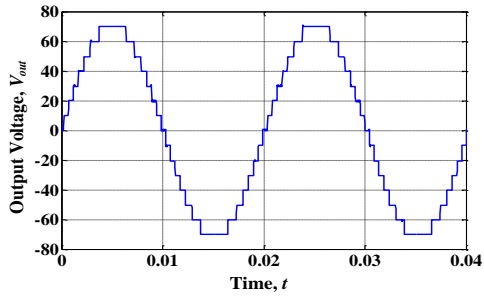
(b) CTB at $m_a = 0.40$



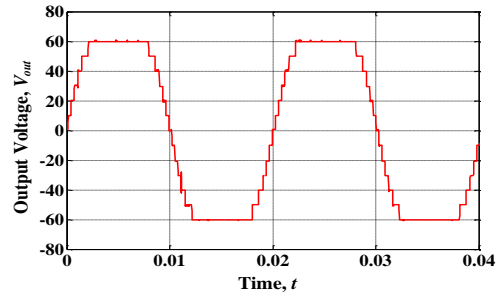
(c) CTA at $m_a = 0.65$



(d) CTB at $m_a = 0.65$



(e) CTA at $m_a = 0.80$



(f) CTB at $m_a = 0.80$

Figure 4. Experimental result of output voltage waveform for CTA and CTB at modulation index 0.40, 0.65 and 0.80



(a) CTA at $m_a = 0.40$



(b) CTB at $m_a = 0.40$



(c) CTA at $m_a = 0.65$



(d) CTB at $m_a = 0.65$



(e) CTA at $m_a = 0.80$



(f) CTB at $m_a = 0.80$

Figure 5. Experimental results of THD and fundamental voltage for CTA and CTB at modulation index 0.40, 0.65, and 0.80

Table 3. Simulation and Experimental Data of 15-level Binary Asymmetric CHBMI

	Modulation Index (m_a)	Simulation Results		Experimental Results	
		Fundamental voltage	THD	Fundamental voltage	THD
		(V_{rms})	(%)	(V_{rms})	(%)
CTA	0.40	25.21	12.75	25.50	12.80
	0.65	41.03	7.31	41.10	7.41
	0.80	50.45	5.34	50.47	5.54
CTB	0.40	25.21	19.65	25.80	19.90
	0.65	41.03	16.13	41.56	16.20
	0.80	50.45	18.80	51.31	18.70

5. CONCLUSION

In this paper, two non-iterative switching-angle calculation techniques (CTA and CTB) applied for a 15-level binary asymmetric CHBMI are proposed and validated via simulation and experiment. Both techniques are able to calculate switching angles for a wider range of modulation index. Based on the simulation and experimental results, CTA has output voltage waveform with lower THD than CTB at the same modulation index. However, CTA is unable to calculate switching angles at the higher range of modulation index, whilst switching angles at that range can be obtained using CTB technique. Hence, both techniques can complement each other to calculate the switching angles for a very wide range of modulation index. Furthermore, the proposed calculation techniques require neither non-transcendental equations nor iterations to obtain the switching angles. Hence, both techniques can be easily extended for other number of levels and CHBMI topologies where a wider range of modulation index is required.

ACKNOWLEDGEMENTS

This research was supported by the School of Electrical System Engineering (UniMAP) and the Ministry of Education Malaysia through the Fundamental Research Grant Scheme (FRGS/2/2014/TK06/UNIMAP/02/3).

REFERENCES

- [1] S. Chatterjee, "A Multilevel Inverter based on SVPWM Technique for Photovoltaic Application," *International Journal of Power Electronics and Drive Systems*, vol/issue: 3(1), pp. 62–73, 2013.
- [2] M. S. Kumar and R. Kannan, "Utilizing the Optimization Algorithm in Cascaded H-Bridge Multilevel Inverter," *TELKOMNIKA Indonesian Journal of Electrical Engineering*, vol/issue: 13(3), pp. 458–466, 2015.
- [3] B. Ozpineci, *et al.*, "Harmonic Optimization of Multilevel Converters using Genetic Algorithms," *IEEE Power Electronics Letters*, vol/issue: 3(3), pp. 92–95, 2005.
- [4] J. N. Chiasson, *et al.*, "A Unified Approach to Solving the Harmonic Elimination Equations in Multilevel Converters," *IEEE Transactions on Power Electronics*, vol/issue: 19(2), pp. 478–490, 2004.
- [5] J. S. Lai and F. Z. Peng, "Multilevel Converters – A New Breed of Power Converters," *IEEE Transactions on Industry Applications*, vol/issue: 32(3), pp. 509–517, 1996.
- [6] E. Babaei, *et al.*, "A Novel Structure for Multilevel Converters," in 2005 International Conference on Electrical Machines and Systems, vol. 2, pp. 1278–1283, 2005.
- [7] E. Babaei, *et al.*, "Reduction of DC Voltage Sources and Switches in Asymmetrical Multilevel Converters using a Novel Topology," *Electric Power Systems Research*, vol/issue: 77(8), pp. 1073–1085, 2007.
- [8] R. Taleb, *et al.*, "Genetic Algorithm Application in Asymmetrical 9-Level Inverter," *International Journal of Power Electronics and Drive Systems*, vol/issue: 7(2), pp. 521–530, 2016.
- [9] L. M. Tolbert, *et al.*, "Multilevel Converter for Large Electric Drives," *IEEE Transactions on Industry Applications*, vol/issue: 35(1), pp. 36–43, 1999.
- [10] Y. L. Kameswari and O. C. Sekhar, "Fuzzy Logic Controlled Harmonic Suppressor in Cascaded Multilevel Inverter," *International Journal of Power Electronics and Drive Systems*, vol/issue: 7(2), pp. 303–310, 2016.
- [11] T. Cunningham, "Cascade Multilevel Inverters for Large Hybrid-Electric Vehicle Applications with Variant DC Sources," M.S. Thesis, University Tennessee, Knoxville, 2001.
- [12] F. L. Luo and H. Ye, "Advanced DC/AC Inverters: Applications in Renewable Energy," Taylor & Francis, 2013.